HHS Public Access

Author manuscript

Exp Dermatol. Author manuscript; available in PMC 2018 May 01.

Published in final edited form as:

Exp Dermatol. 2017 May ; 26(5): 423–430. doi:10.1111/exd.13256.

SVEP1 plays a crucial role in epidermal differentiation

L Samuelov[1,*], **Q Li**[2,*], **R Bochner**[1,*], **N Najor**[3], **L Albrecht**[3], **N Malchin**[1], **T Goldsmith**[1], **M Grafi-Cohen**[1], **D Vodo**[1], **G Fainberg**[1], **B Meilik**[4], **I Goldberg**[1], **E Warshauer**[1], **T Rogers**[1], **S Edie**[5], **A Ishida-Yamamoto**[6], **L Burzenski**[5], **N Erez**[7], **SA Murray**[5], **AD Irvine**[8], **L Shultz**[5], **K Green**[3], **J Uitto**[2], **E Sprecher**[1,9], and **O Sarig**[1]

[1]Department of Dermatology, Tel Aviv Sourasky Medical Center, Tel Aviv, Israel [2]Department of Dermatology and Cutaneous Biology, Sidney Kimmel Medical College, Thomas Jefferson University, Philadelphia, USA [3]Departments of Pathology and Dermatology, Northwestern University Feinberg School of Medicine, Chicago, Illinois, USA [4]Department of Plastic and Reconstructive Surgery, Tel Aviv Sourasky Medical Center, Tel Aviv, Israel [5]The Jackson Laboratory, Bar Harbor, USA [6]Department of Dermatology, Asahikawa Medical University, Asahikawa, Japan [7]The Research Center for Digestive Tract and Liver Diseases, Tel Aviv Sourasky Medical Center, Tel Aviv, Israel [8]Department of Clinical Medicine, Trinity College, Dublin, Ireland [9]Department of Human Molecular Genetics & Biochemistry, Sackler Faculty of Medicine, Tel Aviv University, Ramat Aviv, Israel

Abstract

SVEP1 is a recently identified multi-domain cell adhesion protein, homologous to the mouse polydom protein, which has been shown to mediate cell-cell adhesion in an integrin dependent-manner in osteogenic cells. In the present study, we characterized SVEP1 function in the epidermis. *SVEP1* was found by qRT-PCR to be ubiquitously expressed in human tissues, including the skin. Confocal microscopy revealed that SVEP1 is normally mostly expressed in the cytoplasm of basal and suprabasal epidermal cells. Down-regulation of *SVEP1* expression in primary keratinocytes resulted in decreased expression of major epidermal differentiation markers. Similarly, *SVEP1* down-regulation was associated with disturbed differentiation and marked epidermal acanthosis in three-dimensional skin equivalents. In contrast, the dispase assay failed to demonstrate significant differences in adhesion between keratinocytes expressing normal vs. low levels of SVEP1. Homozygous Svep1 knockout mice were embryonic lethal. Thus, to assess the importance of SVEP1 for normal skin homeostasis *in vivo*, we down regulated *SVEP1* in zebra fish embryos with a *Svep1*-specific splice morpholino. Scanning electron microscopy revealed a rugged epidermis with perturbed microridge formation in the center of the keratinocytes of morphant larvae. Transmission electron microscopy analysis demonstrated abnormal epidermal cell-cell adhesion with disadhesion between cells in *Svep1*-deficient morphant larvae compared to

Corresponding author: Eli Sprecher, Department of Dermatology, Tel Aviv Sourasky Medical Center, 6, Weizmann street, Tel Aviv 64239, Israel, Tel: (972) 3 697 4287, elisp@tlvmc.gov.il.

*Equal contributors

Conflicts of interests

The authors declare no conflicts of interests.

controls. In summary, our results indicate that SVEP1 plays a critical role during epidermal differentiation.

Keywords

SVEP1; integrin α9β1; epidermal differentiation; zebrafish

Introduction

Adhesion molecules play a critical role within the epidermis, responsible for epidermal-dermal junction integrity as well as epidermal barrier function (1, 2). Consequently, abnormal function of these proteins is associated with numerous and mostly severe congenital disorders including various forms of epidermolysis bullosa and disorders of cornification (3).

The SVEP1 gene is located on 9q32, spans 214 kb of genomic DNA and consists of 48 exons, encoding a secreted multi-domain protein which harbors sushi (named also complement control protein; CCP), von Willebrand factor (VWF) type A, epidermal growth factor (EGF) and pentraxin-domain motifs. In addition, it contains additional domains including TNF-receptor cysteine-rich domains, hyaline repeat domains that are involved in cell adhesion, a RGD cell attachment site and a ACR (ADAM disintegrin and metalloproteinase cysteine-rich) domain that plays a role in cell tumorigenesis (4–6). SVEP1 displays more than 80% homology to the mouse polydom protein (5, 7, 8). Recently it has been shown that SVEP1 is an integrin α9β1 ligand with an affinity that far exceeds that of other known integrin α9β1 ligands, and as such it was found to mediate cell-cell adhesion in an integrin dependent-manner in mesenchymal cells. Consistent with these findings, SVEP1 was found to co-localize with integrin α9β1 in mouse tissues *in vivo* (8). The presence of a CCP domain with a selectin super-family signature associated with an EGF domain are reminiscent of the structure of selectins which mediate dynamic cell-cell interactions in several tissues. Accordingly, anti-SVEP1 antibodies were found to perturb cell adhesion in murine bone marrow-derived osteoblastic cells (5).

SVEP1 has been shown to be expressed in murine placenta, lungs, intestine, stomach, skeletal tissue and pre-osteoblastic cells; human, murine and rat bone marrow-derived mesenchymal stem cells; and human placenta, endothelial cells and breast cancer cell lines, while its expression has been shown to be regulated by estrogen and tumor necrosis factor (TNF)-α (4–12). In contrast, the pattern of expression of SVEP1 and its role in human skin remains to be determined. Given the contribution of SVEP1 to the maintenance of cell-cell adhesion in many tissues, and the importance of adhesion molecules for skin function, we characterized SVEP1 expression and function in the epidermis.

Methods

Primary cell cultures

Primary keratinocytes (KCs) and fibroblasts were isolated from adult skin obtained from plastic surgery specimens after having received written informed consent from the donors

according to a protocol reviewed and approved by our institutional review board as previously described (13–15). KCs were maintained in KC Growth Medium (KGM) (Lonza, Walkersville, MD). Fibroblasts were cultured in Dulbecco's Modified Essential Medium (DMEM) supplemented with 20% fetal calf serum (FCS) (Both were purchased from Biological Industries, Beit Haemek, Israel).

siRNA transfection

Primary KCs and fibroblasts were cultured in 100-mm culture plates at 37°C in 5% CO_2 in a humidified incubator and were harvested at 60% confluence. To downregulate *SVEP1* expression, we used Human *SVEP1* small interference RNAs (siRNA) from GE Healthcare Dharmacon (Lafayette, CO), with the following sequences: 5'-GCUACUAUCUAUUGGGUGA-3'; 5'-AGUCUAUAUCGAUGGGAAA-3'; 5'-GGGCAGUGGAGUAGUCCUA-3'; 5'-GUGGAAAGAACGUCGAUGA-3'. As control siRNA, we used Stealth™ RNAi Negative Control Duplex (Invitrogen, Carlsbad, CA). One hundred and eighty pmol of siRNAs were transfected into primary KCs and fibroblasts using Lipofectamine RNAiMax (Invitrogen, Carlsbad, CA). The transfection medium was replaced after 6 hours with KGM (for KCs) or DMEM (for fibroblasts). Seventy-two hours following transfection, the transfected cells were trypsinized and used for organotypic cell cultures as described below.

Organotypic cell cultures

Seventy two hours after transfection, control and SVEP1 knocked-down human fibroblasts were trypsinized, counted and re-suspended in DMEM medium containing 20% FCS (Biological Industries, Beit Haemek, Israel) as previously described (13, 14). Thereafter, 0.1×10^6 fibroblasts per ml of type I Bovine Collagen matrix (Advanced BioMatrix, San Diego, CA) were mixed and 2.5 ml of this solution was poured into 3 μm filter tissue culture inserts (BD, Franklin Lakes, NJ) and allowed to gel for 2 hours at 37°C in a humidified atmosphere according to a protocol modified from Mildner et al. (16). The gels were then equilibrated with KGM (Walkersville, MD, USA) for 2 hours and 1.0×10^6 control or SVEP1 knocked-down human KCs per cm^2 growth area were seeded onto the matrix at a total volume of 2 ml medium per insert. After 24 hours, the system was raised to air-liquid interface and medium was replaced by KC Culture Medium (KCM) as previously described (17). Models were grown for 10 days and medium was changed every other day. For each set of experiments (total of two experiments performed under identical conditions), KCs and fibroblasts were derived from the same donor and used at the third passage. Punch biopsies were obtained from organotypic cell cultures and fixed in 4% paraformaldehyde. Five μm-thick paraffin-embedded sections were processed for hematoxylin eosin staining or immunostaining. RNA was extracted from punch biopsies using RNeasy Fibrous Tissue mini kit (Qiagen, Hilden, Germany).

Quantitative RT-PCR

For quantitative real-time PCR, cDNA was synthesized from 1000 ng of total RNA using qScript kit (Quanta Biosciences, Gaithersburg, MD). cDNA PCR amplification was carried out with the PerfeCTa SYBR Green FastMix (Quanta Biosciences, Gaithersburg, MD) on a StepOnePlus system (Applied Biosystems, Carlsbad, CA) with gene-specific intron-crossing

oligonucleotide pairs (Table S1). Cycling conditions were as follows: 95°C, 30 sec; 95°C, 4 sec; 60°C, 30 sec for 40 cycles. Each sample was analyzed in triplicates. For quantification, standard curves were obtained with serially diluted cDNAs amplified in the same real-time PCR run. Results were normalized to *ACTB, GAPDH* or *PPIA* mRNA levels.

SVEP1 knock-out mice

This strain was generated by the Knockout Mouse Phenotyping Program (KOMP) at the Jackson Laboratory using embryonic stem (ES) cells provided by the International Knockout Mouse Consortium. A knockout-first beta-galactosidase reporter cassette (18) was introduced between exons 7 and 8 of the Svep1 gene, with an additional *loxP* site engineered downstream of exon 8. This cassette was introduced into C57BL/6N-derived JM8.N4 ES cells, and the clone HEPD0747_6_B06 was injected into B6(Cg)- $Tyr^{c\text{-}2J}$/J (Stock No. 58) blastocysts to create chimeras. Following germline transmission, mice were bred to B6N.Cg-Tg(Sox2-cre)1Amc/J mice (Stock No. 014094) to remove the neomycin cassette and exon 8, resulting in a frameshift mutation. Offspring were bred to C57BL/6NJ mice to remove the *cre*-expressing transgene. Mice are maintained on an isogenic C57BL/6NJ (Stock No. 005304) background.

We generated embryos from timed pregnant females and necropsied entire litters at embryonic day 18.5. Embryos were harvested and assessed at embryonic day 18.5 (E18.5), and fixed for three days in 4% paraformaldehyde. Skin from the trunk was removed and processed for histology.

SVEP1 knock down in zebrafish and morphant analysis

Adult wild-type zebrafish were maintained under standard conditions at 28.5°C. Zebrafish embryos and larvae were also maintained at 28.5°C in embryo medium (19). All animals were housed in the zebrafish facility at Thomas Jefferson University and were cared for and used in accordance with Institutional Animal Care and Use Committee guidelines. Standard control morpholino (scMO) (5′-CCTCTTACCTCAGTTACAATTTATA-3’) or Svep1-specific splice (5′-AACCCCGCCCTTTCTTTCTCACTTC-3’) morpholino oligonucleotides were obtained from Gene Tools, LLC (Corvalis, OR). Embryos at the one- to two-cell stage were injected with the morpholinos using glass microelectrodes fitted to a gas pressure injector (PL1-100, Harvard Apparatus). Electrodes were pulled (P-97, Flaming/Brown) and filled with morpholino and phenol red (final concentration 0.025%) to visualize the injected embryos. Control and morphant larvae at 3 days post fertilization (dpf) were processed for scanning or electron microscopy as previously described (19). Specimens were imaged in a JEOL-T330A scanning electron microscope (JEOL, Tokyo, Japan) at 15 kV or a JEOL JEM-1010 transmission electron microscope fitted with a Hamamatsu digital camera (Hamamatsu Photonics, Hamamatsu City, Japan) and AMT Advantage image capture software (AMT, Danvers, MA).

Immunohistochemistry

For SVEP1 immunofluorescence analysis of skin biopsies, 5 μm paraffin-embedded sections were baked overnight at 37°C and de-paraffinized using xylene/ethanol. Antigen retrieval was accomplished using 0.01 M citrate buffer, pH 6.0. Sections were blocked with 2% BSA

in PBS for 30 min at room temperature. Rabbit anti human SVEP1 primary antibody (Abcam, Cambridge, MA) was diluted 1:30 with 2% BSA in PBS and incubated overnight at 4°C. Rhodamine goat anti rabbit IgG (Invitrogen, Carlsbad, CA) was used as a secondary antibody and was diluted 1:200 with 2% BSA in PBS and was incubated for 45 min at room temperature. Coverslips were mounted in DAPI Fluoromount-G (Southern Biotechnologies, Birmingham, AL). Negative control was obtained by omitting the primary antibody. As a positive control, we used a normal placenta tissue (5) which stained positively with the antibody (Fig. S1). Samples were examined using either a Nikon 50I microscope connected to DS-RI1 digital camera or a Zeiss LSM700 confocal microscope for fluorescence image acquisition.

Immunostaining with mouse anti human Ki-67 antibody (DAKO, Hamburg, Germany) was performed as previously described (20).

Immunostaining of KCs and fibroblasts

KCs and fibroblasts that were harvested from punch biopsies were grown on glass coverslips and fixed with 4% paraformaldehyde. Following permeabilization with 0.5% Triton/PBS, slides were blocked in 3% BSA, 2% normal goat serum and 0.2% triton in PBS for 20 min at room temperature. Rabbit anti human SVEP1 primary antibody (Abcam, Cambridge, MA) was diluted 1:30 in blocking solution. The cells were incubated for 1h at room temperature. The cells were then incubated for 45 min at room temperature with a secondary antibody consisting of rhodamine goat anti rabbit IgG (Invitrogen, Carlsbad, CA) diluted 1:200 in PBS. Following several washing steps, coverslips were mounted in DAPI Fluoromount-G (Southern Biotechnologies, Birmingham, AL).

Cell cycle analysis

For cell-cycle analysis, primary KCs were seeded in 6-well plates ($2{\cdot}10^6$ per plate), transfected with 30 pmole of control siRNA (Invitrogen, Carlsbad, CA) or *SVEP1* siRNA (GE Healthcare Dharmacon, Lafayette, CO) for 72h and harvested with trypsin (Biological Industries, Beit Haemek, Israel). The suspensions were centrifuged at 1200 rpm for 5 minutes at room temperature. Pellets were washed once with cold PBS, re-suspended in 500 μl cold PBS, and fixed by adding 5 ml of 70% ethanol. After 1 hour of incubation at 4°C, fixed cells were centrifuged at 1200 rpm for 10 minutes at 4°C, supernatant was discarded and cells were washed with PBS followed by another centrifugation. Then, cells were re-suspended in 500 μl PBS containing RNase A (50 μg/ml) and 0.1% Triton (Sigma-Aldrich, St. Louis, MO) and incubated for 1 hour at 37°C. Cells were stained with propidium iodide (15 μg/ml) (Sigma-Aldrich, St. Louis, MO) and examined by flow cytometry. Flow cytometry was performed on a 3-laser Canto-II flow cytometer (BD, Biosciences, San Jose, CA) instrument and data were analyzed using FACSDiva (V 6.1.3) to determine the relative amounts of cell-cycle phases.

Dispase assay

Electroporation of human foreskin KCs was performed using 50 nm siRNA targeting desmoplakin (DP) (Life Technologies, Grand Island, NY), SVEP1 (Dharmacon, Lafayette, CO), or a scrambled control siRNA (Dharmacon, Lafayette, CO). DP was used as a positive

control for decreased intercellular adhesion. Seventy-two hours following siRNA transfection, cell monolayers were seeded in triplicate into 6-well plates. Twenty-four hours after reaching confluency, cultures were washed twice in Dulbecco's PBS (DPBS) and then incubated in 2 ml of dispase (2.4 U/ml; Roche Diagnostics GmbH, Indianapolis, IN) for 30 min (21, 22). Released monolayers were subjected to mechanical stress to induce fragmentation. Fragments were counted using a dissecting microscope (MZ6; Leica, Buffalo Grove, IL).

Results

SVEP1 is ubiquitously expressed in normal human tissues

Since SVEP1 normal expression was previously investigated mostly in cell lines and murine tissues (4–6, 9–11), we initially assessed its normal expression in human tissues. Using qRT-PCR, we observed ubiquitous expression of *SVEP1* in a wide array of normal human tissues, with maximal expression in the placenta (Fig. 1a). Of note, strong expression was also demonstrated in human epidermal KCs and skin fibroblasts (Fig. 1b). This is in line with previous studies in mice demonstrating ubiquitous expression of the full length polydom gene transcript in different tissues (4).

We then established the protein expression pattern of SVEP1 in human skin. Immunostaining showed that although SVEP1 immunoreactivity was seen throughout the human epidermis, it is most prominently expressed in the basal and lower suprabasal layers of the epidermis. In addition, prominent expression of SVEP1 was shown in dermal fibroblasts residing in the upper dermis (Fig.1 c–d).

In primary epidermal KCs and fibroblasts cell cultures from healthy individuals, SVEP1 expression was most prominent in the nuclear and peripheral cytoplasmic compartments of the cells (Fig.1 e–f; Fig S2). This contrasts with previous reports that demonstrated cell membrane and cytoplasmic immunoreactivity in other cell lines (5).

SVEP1 silencing in primary KCs is associated with abnormal expression of differentiation-associated genes

To examine the possibility that SVEP1 expression in the skin may reflect a role for this protein during epidermal ontogenesis, we knocked down primary human KCs for *SVEP1* and assessed the effect of decreased SVEP1 expression on various epidermal differentiation-associated genes. SVEP1-silenced KCs showed downregulation of the differentiation-associated keratins (*KRT1* and *KRT10)* (23) and upregulation of *TGM1* encoding transglutaminase 1, while there was no significant difference in the expression of the proliferation-associated keratin genes *KRT5, KRT14* and *KRT6*a (23), at the mRNA level (Fig. 2a).

Human skin equivalents silenced for SVEP1 show acanthosis and abnormal expression of differentiation markers

Because *SVEP1* down-regulation in keratinocyte cell cultures seemed to result in abnormal regulation of differentiation-associated genes, we hypothesized that it may be involved in

epidermal differentiation. To assess this possibility, we established a *SVEP1*-silenced organotypic three dimensional skin model (Fig. S3). *SVEP1*-silenced organotypic skin model displayed a significantly thicker epidermis (acanthosis), with no evidence of abnormal cell-cell adhesion, compared to control skin models (Fig. 2b–d). In line with these results, there was no significant difference in the expression of several adhesion markers between *SVEP1*-silenced and control organotypic skin models (Fig. S4). In addition, *SVEP1* silencing resulted in abnormal RNA expression of differentiation-associated markers compared to control skin models (Fig. 2e). In contrast to the findings in *SVEP1*-silenced primary KCs, *SVEP1* silenced skin equivalents revealed slight but significant reduction in the expression of the *KRT5* and *KRT6a* as well while the expression of *KRT14* was not significantly affected (Fig. 2e). Given the fact that skin models were grown for 10 days prior to obtaining skin biopsies, no evidence of proliferative cells was documented by Ki67 staining in both control and *SVEP1*-deficient skin models (data not shown). We therefore used cell cycle FACS analysis to ascertain the effect of SVEP1 down-regulation on KCs proliferation. We found that keratinocytes downregulated for *SVEP1* do not demonstrate significant changes in proliferation indices compared to control siRNA-treated keratinocytes (Fig. S5).

Svep1 knock-down in a Zebrafish model reveals abnormal epidermal morphology and disadhesion of epidermal cells

To assess the importance of SVEP1 for normal skin homeostasis *in vivo*, we studied a *Svep1*-null mouse model generated through the KOMP^2 program at The Jackson Laboratory (*Svep1*$^{tm1b(EUCOMM)Hmgu}$/J). *Svep1*-null mice were found to be embryonic lethal, with no homozygous null animal identified at wean (n=98). *Svep1*-null embryos were obtained via heterozygous crosses at E18.5. Mutant embryos showed gross morphological abnormalities including edema, abnormal skin coloration and tail/limb abnormalities. In line with the results in organotypic skin models, skin biopsies of these embryos revealed significantly thicker epidermal layer compared to heterozygous controls (Fig. S6).

Because we could not study adult *Svep1*-null mice, we down regulated *Svep1* in zebrafish embryos with a *Svep1*-specific splice morpholino (Fig. 3a). RT-PCR of total RNA extracted from zebrafish 3 days after morpholino injection revealed that essentially all (>90%) of the *Svep1* pre-mRNA remained unprocessed, attesting to the efficiency of the morpholino knockdown (Fig.3b). Injection of standard control morpholino (scMO) did not affect *Svep1* pre-mRNA splicing (Fig.3b). Scanning electron microscopy showed that the morphant larvae injected with a splice morpholino for *Svep1* gene displays rugged morphology of the epidermis with perturbed micro-ridge formation in the center of the KCs. This was in contrast to the standard control morpholino injected control larvae that demonstrated well-demarcated KCs with normal microridges at the cell-cell borders (Fig. 3c–d). Transmission electron microscopy analysis demonstrated abnormal epidermal cell-cell adhesion with disadhesion between cells (but normal appearing desmosomes) in *Svep1* morphant larvae compared to control (Fig. 3e).

SVEP1-deficient human epidermal monolayers reveal normal cell-cell adhesion

Given the abnormal epidermal cell adhesion observed in *Svep1*-deficient morphant larvae, we aimed at determining the role of SVEP1 in cell-cell adhesion in human keratinocytes. We therefore conducted a dissociation assay in epidermal monolayers generated from *SVEP1*-specific siRNA- and control siRNA-transfected KCs (Fig. S7). We observed that the loss of SVEP1 did not result in an adhesion defect in keratinocytes as determined by a dispase assay (Fig. 4). While we cannot rule out that a more complete *SVEP1* knockdown would have a detrimental impact on adhesion, the level of adhesion in keratinocytes was significantly reduced upon knockdown of the obligate desmosome component, DP (Fig. 4).

Discussion

Here we provide the first evidence that SVEP1, a recently identified integrin α9β1 ligand, is expressed in normal human skin and plays a hitherto unknown role during epidermal differentiation.

SVEP1 expression was previously investigated mostly in cell lines and murine tissues while here we provide the first evidence that SVEP1 is normally expressed in a wide array of human tissues with relatively high level of expression in human skin. Recently, several studies demonstrated the significant role played by SVEP1 in systemic conditions. A missense variant in the *SVEP1* gene was associated with an increased risk of coronary artery disease in association with type 2 diabetes and higher systolic and diastolic blood pressure (24). Moreover, a polymorphism in the *SVEP1* gene was associated with altered 28-day mortality of septic shock and SVEP1 knockdown in a cellular model of sepsis influenced several inflammatory processes (25). In line with these findings, *SVEP1* gene expression was increased in an vitro cell culture model of endotoxemia (12).

Integrin α9β1 is known to bind a panel of extracellular matrix (ECM) proteins, including tenascin-C, osteopontin, fibronectin isoform containing an EIIIA domain, membrane proteins (ADAM proteases and VCAM-1) and growth factors (VEGF and NGF) (26–32). Polydom was shown to bind integrin α9β1 ligand *in vivo* with higher affinity than that of known ligands including tenascin-C (8). Here, we show that SVEP1 deficiency affects epidermal differentiation. Of interest, another integrin α9β1 ligand, EMILIN1 (33), was shown to affect epidermal cell proliferation, possibly through direct binding to integrin α9β1 (known to be expressed on basal KCs) and activation of the Erk1/2 and Akt/PI3K pathways (33). Of interest, although SVEP1 was shown to be present throughout the entire epidermis, it was more prominently expressed in the basal and lower suprabasal layers of the epidermis as well as in upper dermal fibroblasts. This observation is reminiscent of the pattern of expression of integrin α9β1 which SVEP1 binds. Integrin α9β1 has been shown to mediate activation of the ERK signaling pathway (34, 35) while attenuation of the latter has been shown to promote epidermal differentiation (36, 37). Collectively, these data suggest that the effect of SVEP1 on epidermal differentiation may involve SVEP1 binding to integrin α9β1.

Regardless of its exact mechanism of action, SVEP1 expression was found to be required for the normal expression of differentiation-associated genes. Its absence in both *in vitro* (human tri-dimensional cultures) and *in vivo* (mice and zebrafish knockdown experiments)

models resulted in perturbed epidermal differentiation. SVEP1 has been shown to regulate cell-cell adhesion in human bone tissues (8) and SVEP1 knockdown in a cellular model of sepsis altered the expression of mediators of leukocyte adhesion to the vascular endothelium (25). Consistent with this observation, blisters were observed in SVEP1 knocked down zebrafish larvae. However, no evidence for abnormal intercellular adhesion was observed in human skin equivalents, mice model or in keratinocyte monolayers, while both *SVEP1*-defficient organotypic skin models and *Svep1*-null mice revealed significant acanthosis compared to controls. The fact that SVEP1 seems to affect epidermal differentiation in all models but is apparently not required for normal cell-cell adhesion in mammalian systems suggest that these two functions are not related. Alternatively, we cannot rule out that perturbation of cell-cell adhesion is dependent on the degree of SVEP1 down-regulation which may vary from one model to the other.

Taken together, our study identifies for the first time a role for SVEP1 in the regulation of epidermal differentiation. Whether its activity is mediated by binding to integrin α9β1 or another receptor remains to be determined.

Supplementary Material

Refer to Web version on PubMed Central for supplementary material.

Acknowledgments

This study was supported by a generous donation of Israel and Ruth Ram, by the National Institutes of Health (R37 AR043380, RO1 AR041836, R01 CA122151) and J.L. Mayberry Endowment (KJG), the National Institutes of Health F32AR066465 (NN), and the American Heart Association Fellowship 14PRE20380540 (LVA).

LS participated in the design of the experiments and the writing of the manuscript, performed experiments and analyzed the data; QL designed and performed the experiments in zebrafish model and analyzed the data; RB participated in the design of the experiments and the writing of the manuscript, performed experiments and analyzed the data; NN performed the experiments in epidermal monolayers and analyzed the data; LA performed the experiments in epidermal monolayers and analyzed the data; NM performed experiments and analyzed the data; TG performed experiments and analyzed the data; MGC performed experiments and analyzed the data; DV performed experiments and analyzed the data; GF performed experiments and analyzed the data; EW performed experiments and analyzed the data; TR performed experiments and analyzed the data; SE performed the experiments in knocked-out mice and analyzed the data; AIY performed experiments and analyzed the data; LB performed the experiments in knocked-out mice and analyzed the data; NE performed confocal microscopy experiments and analyzed the data; BM performed the plastic surgeries from which skin was obtained and used for generation of keratinocytes and fibroblasts cell cultures and skin equivalents; IG supervised the research program, contributed to the design of the experiments; SAM performed and supervised the experiments in knocked-out mice and analyzed the data; ADI supervised the research program, contributed to the design of the experiments; LS supervised the research program, contributed to the design of the experiments; KJG conceived and designed the experiments and analyzed the data; JU conceived and designed the experiments and analyzed the data; ES jointly supervised the project, conceived and designed the experiments, analyzed the data and participated to the writing of the paper; OS jointly supervised the research, participated to the design of the experiments and the writing of the manuscript, performed experiments and analyzed the data.

References

1. Sumigray KD, Lechler T. Cell adhesion in epidermal development and barrier formation. Current topics in developmental biology. 2015; 112:383–414. [PubMed: 25733147]
2. Simpson CL, Patel DM, Green KJ. Deconstructing the skin: cytoarchitectural determinants of epidermal morphogenesis. Nature reviews Molecular cell biology. 2011; 12:565–580. [PubMed: 21860392]

3. Samuelov L, Sprecher E. Inherited desmosomal disorders. Cell and tissue research. 2015; 360:457–475. [PubMed: 25487406]
4. Glait-Santar C, Pasmanik-Chor M, Benayahu D. Expression pattern of SVEP1 alternatively-spliced forms. Gene. 2012; 505:137–145. [PubMed: 22659106]
5. Shur I, Socher R, Hameiri M, et al. Molecular and cellular characterization of SEL-OB/SVEP1 in osteogenic cells in vivo and in vitro. Journal of cellular physiology. 2006; 206:420–427. [PubMed: 16206243]
6. Shur I, Zemer-Tov E, Socher R, et al. SVEP1 expression is regulated in estrogen-dependent manner. Journal of cellular physiology. 2007; 210:732–739. [PubMed: 17139625]
7. Gilges D, Vinit MA, Callebaut I, et al. Polydom: a secreted protein with pentraxin, complement control protein, epidermal growth factor and von Willebrand factor A domains. Biochem J. 2000; 352(Pt 1):49–59. [PubMed: 11062057]
8. Sato-Nishiuchi R, Nakano I, Ozawa A, et al. Polydom/SVEP1 is a ligand for integrin alpha9beta1. The Journal of biological chemistry. 2012; 287:25615–25630. [PubMed: 22654117]
9. Shefer G, Benayahu D. SVEP1 is a novel marker of activated pre-determined skeletal muscle satellite cells. Stem cell reviews. 2010; 6:42–49. [PubMed: 20052625]
10. Glait-Santar C, Benayahu D. SVEP1 promoter regulation by methylation of CpG sites. Gene. 2011; 490:6–14. [PubMed: 21963386]
11. Glait-Santar C, Benayahu D. Regulation of SVEP1 gene expression by 17beta-estradiol and TNFalpha in pre-osteoblastic and mammary adenocarcinoma cells. The Journal of steroid biochemistry and molecular biology. 2012; 130:36–44. [PubMed: 22265959]
12. Schwanzer-Pfeiffer D, Rossmanith E, Schildberger A, et al. Characterization of SVEP1, KIAA, and SRPX2 in an in vitro cell culture model of endotoxemia. Cellular immunology. 2010; 263:65–70. [PubMed: 20236627]
13. Fuchs-Telem D, Stewart H, Rapaport D, et al. CEDNIK syndrome results from loss-of-function mutations in SNAP29. The British journal of dermatology. 2011; 164:610–616. [PubMed: 21073448]
14. Nousbeck J, Ishida-Yamamoto A, Bidder M, et al. IGFBP7 as a potential therapeutic target in Psoriasis. The Journal of investigative dermatology. 2011; 131:1767–1770. [PubMed: 21562573]
15. Samuelov L, Sarig O, Harmon RM, et al. Desmoglein 1 deficiency results in severe dermatitis, multiple allergies and metabolic wasting. Nature genetics. 2013; 45:1244–1248. [PubMed: 23974871]
16. Mildner M, Ballaun C, Stichenwirth M, et al. Gene silencing in a human organotypic skin model. Biochemical and biophysical research communications. 2006; 348:76–82. [PubMed: 16875670]
17. I L, F W. Keratinocyte Methods. 1994:9–15.
18. Skarnes WC, Rosen B, West AP, et al. A conditional knockout resource for the genome-wide study of mouse gene function. Nature. 2011; 474:337–342. [PubMed: 21677750]
19. Li Q, Frank M, Akiyama M, et al. Abca12-mediated lipid transport and Snap29-dependent trafficking of lamellar granules are crucial for epidermal morphogenesis in a zebrafish model of ichthyosis. Disease models & mechanisms. 2011; 4:777–785. [PubMed: 21816950]
20. Samuelov L, Sprecher E, Tsuruta D, et al. P-cadherin regulates human hair growth and cycling via canonical Wnt signaling and transforming growth factor-beta2. The Journal of investigative dermatology. 2012; 132:2332–2341. [PubMed: 22696062]
21. Hobbs RP, Green KJ. Desmoplakin regulates desmosome hyperadhesion. The Journal of investigative dermatology. 2012; 132:482–485. [PubMed: 21993560]
22. Hudson TY, Fontao L, Godsel LM, et al. In vitro methods for investigating desmoplakin-intermediate filament interactions and their role in adhesive strength. Methods in cell biology. 2004; 78:757–786. [PubMed: 15646638]
23. Freedberg IM, Tomic-Canic M, Komine M, et al. Keratins and the keratinocyte activation cycle. The Journal of investigative dermatology. 2001; 116:633–640. [PubMed: 11348449]
24. Myocardial Infarction G; Investigators C A E C. Coding Variation in ANGPTL4, LPL, and SVEP1 and the Risk of Coronary Disease. The New England journal of medicine. 2016; 374:1134–1144. [PubMed: 26934567]

25. Nakada TA, Russell JA, Boyd JH, et al. Identification of a nonsynonymous polymorphism in the SVEP1 gene associated with altered clinical outcomes in septic shock. Critical care medicine. 2015; 43:101–108. [PubMed: 25188548]

26. Eto K, Huet C, Tarui T, et al. Functional classification of ADAMs based on a conserved motif for binding to integrin alpha 9beta 1: implications for sperm-egg binding and other cell interactions. The Journal of biological chemistry. 2002; 277:17804–17810. [PubMed: 11882657]

27. Liao YF, Gotwals PJ, Koteliansky VE, et al. The EIIIA segment of fibronectin is a ligand for integrins alpha 9beta 1 and alpha 4beta 1 providing a novel mechanism for regulating cell adhesion by alternative splicing. The Journal of biological chemistry. 2002; 277:14467–14474. [PubMed: 11839764]

28. Smith LL, Cheung HK, Ling LE, et al. Osteopontin N-terminal domain contains a cryptic adhesive sequence recognized by alpha9beta1 integrin. The Journal of biological chemistry. 1996; 271:28485–28491. [PubMed: 8910476]

29. Staniszewska I, Sariyer IK, Lecht S, et al. Integrin alpha9 beta1 is a receptor for nerve growth factor and other neurotrophins. Journal of cell science. 2008; 121:504–513. [PubMed: 18230652]

30. Taooka Y, Chen J, Yednock T, et al. The integrin alpha9beta1 mediates adhesion to activated endothelial cells and transendothelial neutrophil migration through interaction with vascular cell adhesion molecule-1. The Journal of cell biology. 1999; 145:413–420. [PubMed: 10209034]

31. Vlahakis NE, Young BA, Atakilit A, et al. The lymphangiogenic vascular endothelial growth factors VEGF-C and -D are ligands for the integrin alpha9beta1. The Journal of biological chemistry. 2005; 280:4544–4552. [PubMed: 15590642]

32. Yokosaki Y, Palmer EL, Prieto AL, et al. The integrin alpha 9 beta 1 mediates cell attachment to a non-RGD site in the third fibronectin type III repeat of tenascin. The Journal of biological chemistry. 1994; 269:26691–26696. [PubMed: 7523411]

33. Danussi C, Petrucco A, Wassermann B, et al. EMILIN1-alpha4/alpha9 integrin interaction inhibits dermal fibroblast and keratinocyte proliferation. The Journal of cell biology. 2011; 195:131–145. [PubMed: 21949412]

34. Gupta SK, Vlahakis NE. Integrin alpha9beta1: Unique signaling pathways reveal diverse biological roles. Cell adhesion & migration. 2010; 4:194–198. [PubMed: 20179422]

35. Sun X, Fa P, Cui Z, et al. The EDA-containing cellular fibronectin induces epithelial-mesenchymal transition in lung cancer cells through integrin alpha9beta1-mediated activation of PI3-K/AKT and Erk1/2. Carcinogenesis. 2014; 35:184–191. [PubMed: 23929437]

36. Eckert RL, Efimova T, Dashti SR, et al. Keratinocyte survival, differentiation, and death: many roads lead to mitogen-activated protein kinase. The journal of investigative dermatology Symposium proceedings / the Society for Investigative Dermatology, Inc [and] European Society for Dermatological Research. 2002; 7:36–40.

37. Harmon RM, Simpson CL, Johnson JL, et al. Desmoglein-1/Erbin interaction suppresses ERK activation to support epidermal differentiation. The Journal of clinical investigation. 2013; 123:1556–1570. [PubMed: 23524970]

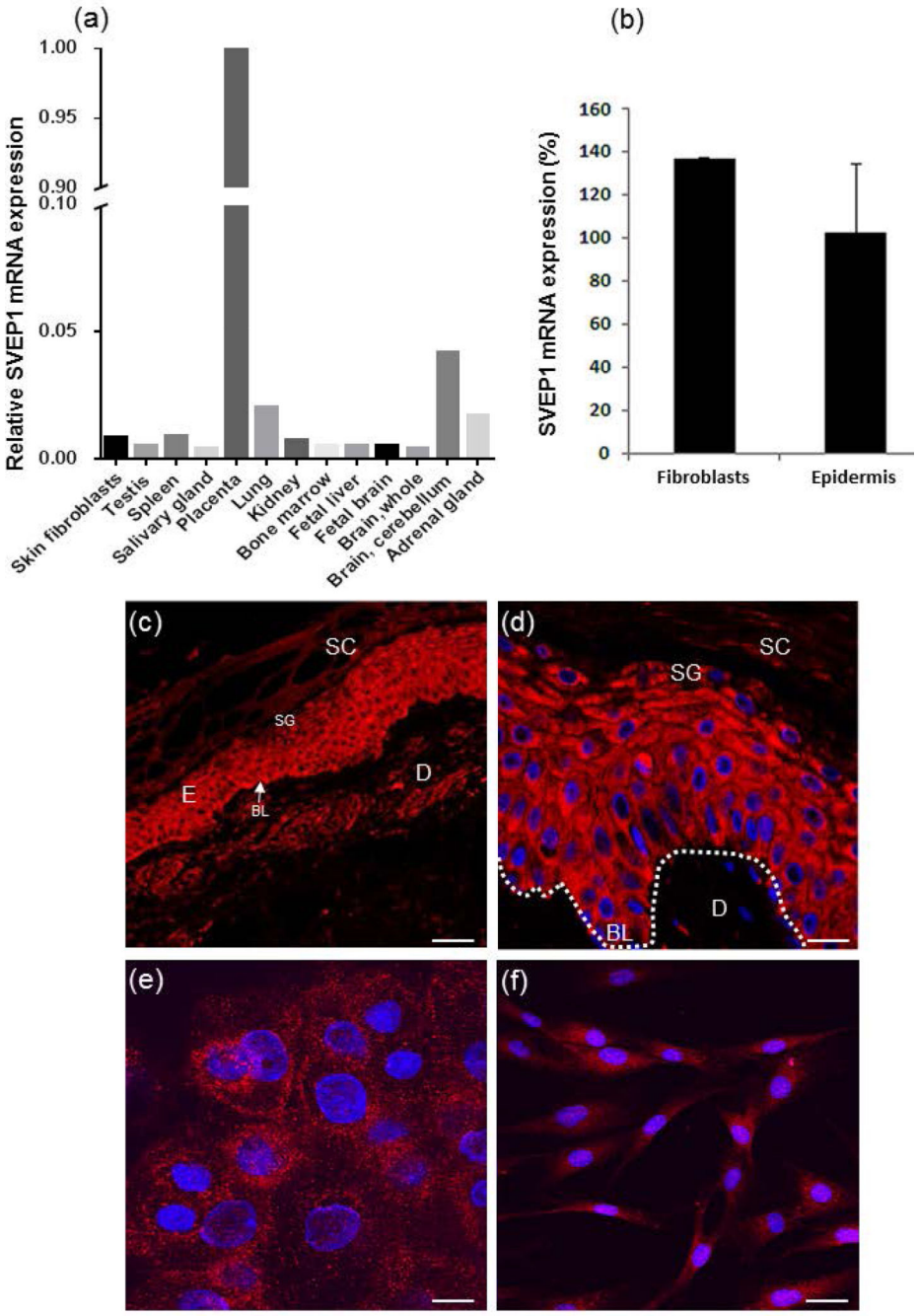

Figure 1. SVEP1 expression in human tissues

(a) *SVEP1* mRNA expression was evaluated using qRT-PCR in normal human tissues. Results are expressed as relative to gene expression in the placenta normalized to *ACTB* RNA levels; **(b)** *SVEP1* mRNA expression in cultured human KCs and fibroblasts. Results are expressed as % of expression relative to keratinocytes and are normalized to *ACTB* RNA levels; **(c)** SVEP1 immunostaining of skin biopsies obtained from healthy individual reveals SVEP1 expression in all epidermal layers and in dermal fibroblasts residing in the upper dermis; **(d)** A higher magnification demonstrates increased expression of SVEP1 in the basal

and suprabasal layers of the epidermis (bars; c = 100μm, d = 40μm). Dotted lines represent epidermal-dermal junction and localization of the basement membrane; E-epidermis; D-dermis; SC-stratum corneum; SG-stratum granulosum; BL-basal layer; **(e–f)** KCs (e) and fibroblasts (f) isolated from skin biopsies obtained from healthy individuals demonstrate SVEP1 expression most prominent in the peripheral cytoplasmic and nuclear compartments of the cells (bar = 40 μm).

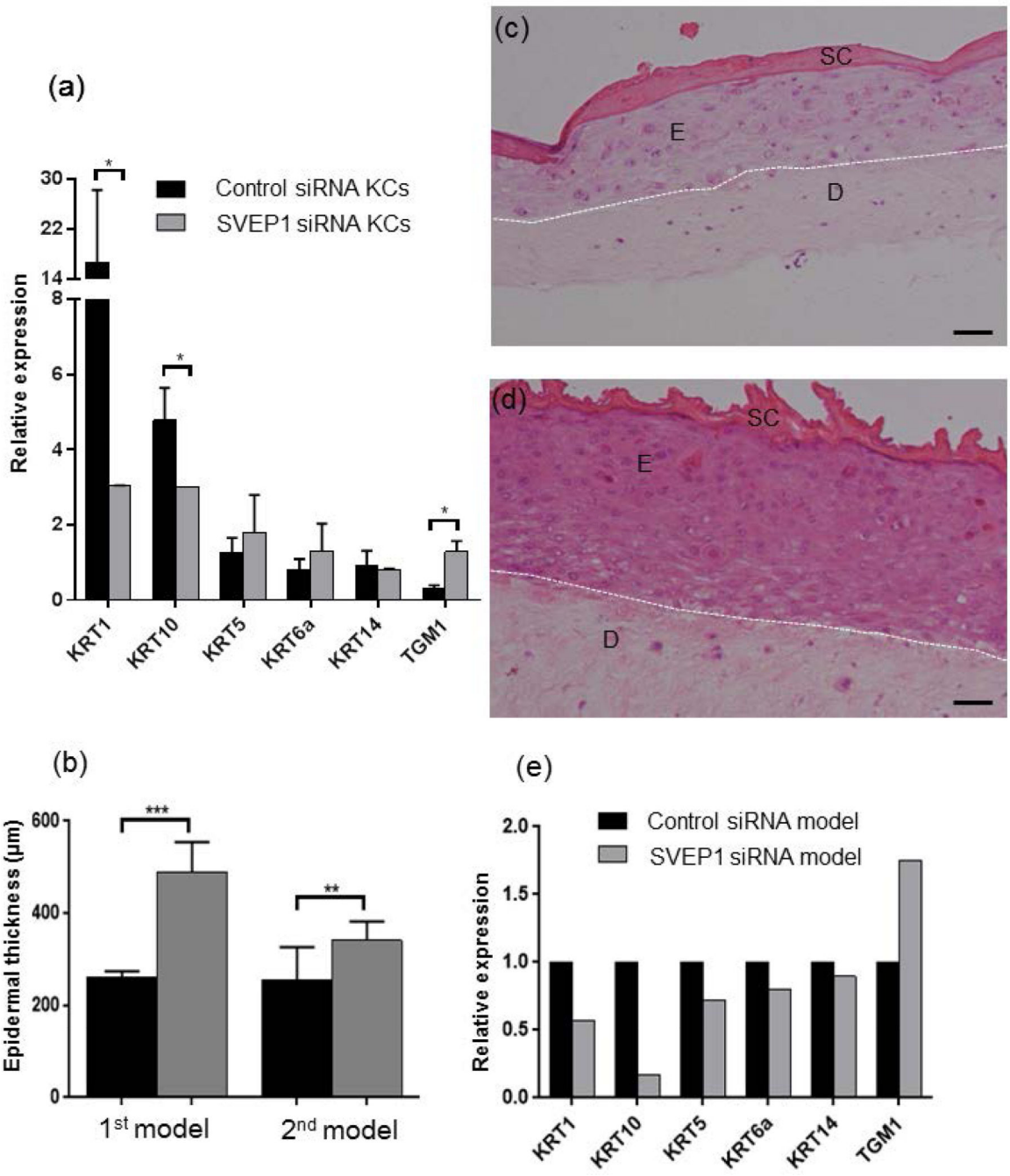

Figure 2. SVEP1 knockdown in primary KCs and organotypic cell cultures

(a) Gene expression was assessed by qRT-PCR in *SVEP1*-silenced primary KCs (KCs) compared to control small interfering RNA (siRNA) treated KCs. Following siRNA transfection, KCs were cultured with and without calcium (1.5mM) for 96 hours. Results are expressed as relative gene expression in KCs cultured at high vs. low calcium concentration (t-test; *p<0.05). Results were normalized to *GAPDH* RNA levels; **(b–e)** Human primary KCs and fibroblasts transfected with *SVEP1* siRNA or control siRNA were used to generate skin equivalents. The experiment was repeated twice under identical conditions (the results

of the first experiment are designated as "1st model" while the results of the second experiment are designated as "2nd model"). Punch biopsies were obtained from skin equivalents at day 10 and stained for hematoxylin and eosin (H&E; bar = 50μm). Epidermal thickness was evaluated in *SVEP1*-deficient and control siRNA treated skin equivalents, in both experiments (b). Note significant acanthosis in skin equivalents downregulated for *SVEP1* (d) compared to control (c). Dotted lines represent epidermal-dermal junction. E-epidermis; D-dermis; SC-stratum corneum; (e)RNA was extracted from punch biopsies derived from skin equivalents and gene expression was assessed using qRT-PCR. Results are expressed gene expression in down-regulated skin equivalents relative to control skin equivalents. Data were normalized to *GAPDH* RNA levels (t-test; *$p<0.05$, **$p<0.01$.

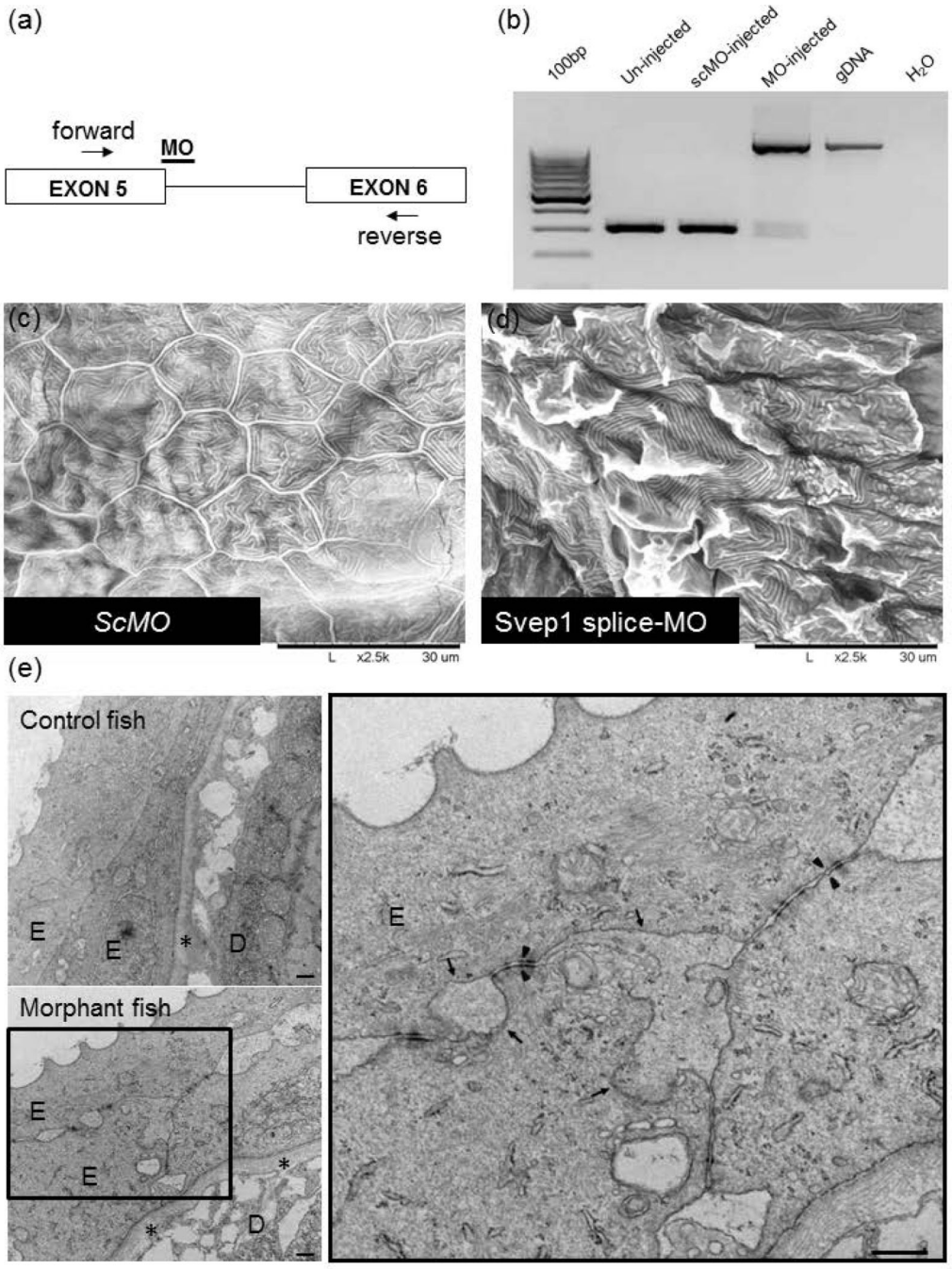

Figure 3. Svep1 knockdown in a zebrafish model

(a–b) Knockdown of *Svep1* by a splice site morphilino (MO). The morpholino targets the splice donor site at the exon 5/intron 5 border of zebrafish *Svep1* gene (a). The consequences of MO on *Svep1* pre-mRNA processing was determined by RT-PCR using primers located in exons 5 and 6 (b). scMO-standard control morpholino; gDNA-genomic DNA; **(c–d)** Scanning electron microscopy analysis of the skin of the tail of a control larvae injected with the global standard control morpholino (scMO) shows the presence of KCs with well-demarcated cell-cell borders and containing microridges (c) while the morphant

larvae injected with a splice site morpholino for *Svep1* gene reveals rugged epidermis with perturbed microridge formation in the center of the KCs (d); **(e)** Transmission electron microscopy demonstrates abnormal epidermal cell-cell adhesion with disadhesion between the cells in the *Svep1* morphant larvae compared to control. Arrows mark the separation of cell-cell contacts while asterisks mark the basement membrane. Arrowheads point to the presence of normal appearing desmosomes. (bar= 500nm). E-epidermis; D-dermis.

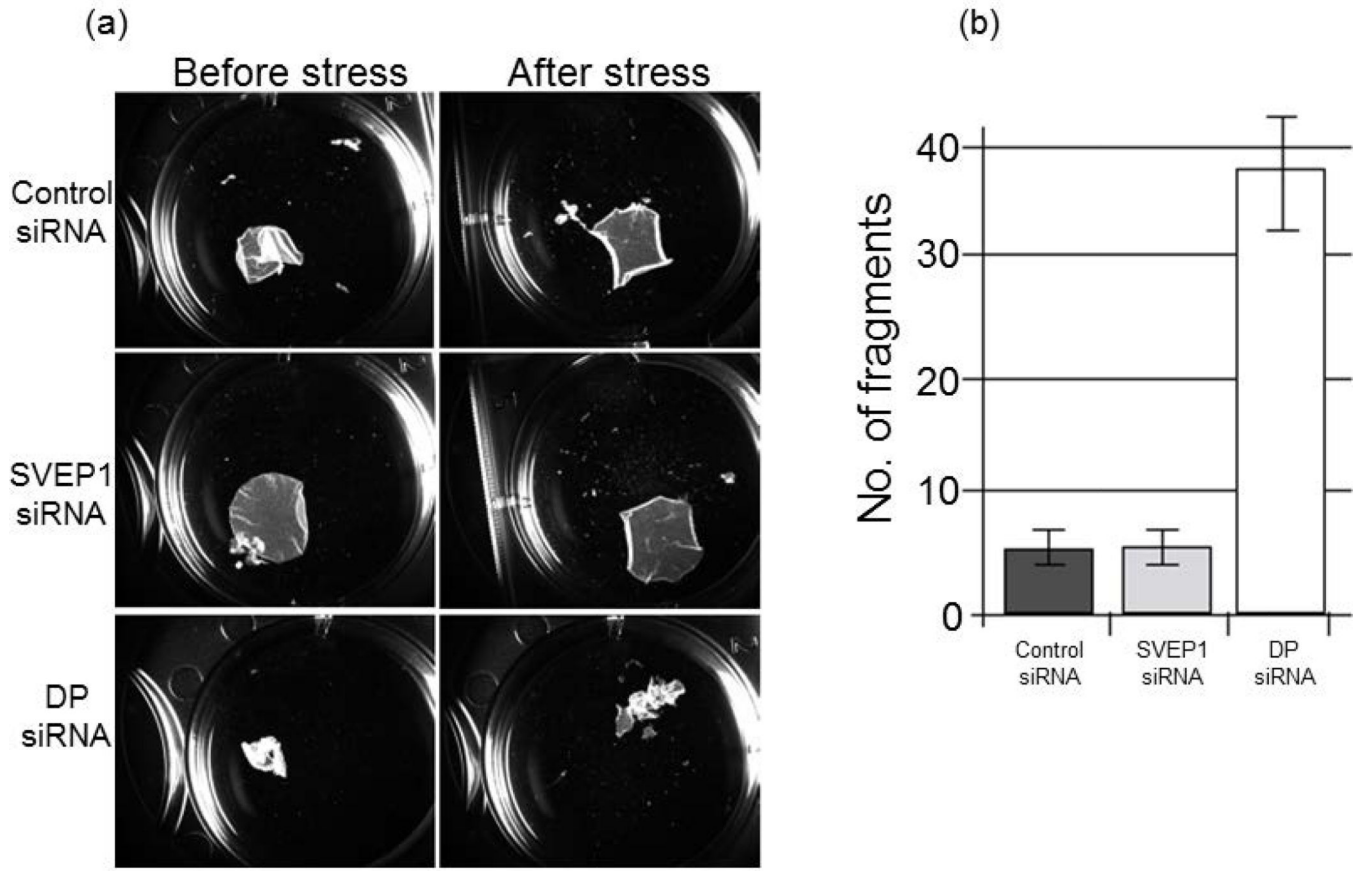

Figure 4. Intact intercellular adhesion in epithelial sheets in the absence of SVEP1

(a) Electroporation of normal human foreskin-derived keratinocytes was performed using siRNA targeting *SVEP1, DSP* encoding desmoplakin (DP) or a scrambled control siRNA. DP is used as a positive control for decreased intercellular adhesion. 72 h following siRNA treatment, cell monolayers were seeded in triplicate into 6-well plates. 24 h after reaching confluency, cultures were washed twice in DPBS and then incubated in 2 ml of dispase (2.4 U/ml) for 30 min; **(b)** Released monolayers were subjected to mechanical stress to induce fragmentation. Quantification of the number of total particles in each well between each condition is shown as an average from the triplicate wells after stress. Fragments were counted using a dissecting microscope (MZ6; Leica). Results are representative of three experiments each performed in triplicate.